THE JOURNAL OF PHYSICAL CHEMISTRY LETTERS
A JOURNAL OF THE AMERICAN CHEMICAL SOCIETY

pubs.acs.org/JPCL

Letter

Terahertz Signatures of the Methane Replacement Reaction in Hydroquinone Clathrates

Katharine D. Bancroft,* Saheed A. Ajibade, Johanna Kölbel, Michael T. Ruggiero, and Daniel M. Mittleman

Cite This: *J. Phys. Chem. Lett.* 2024, 15, 6092−6098

Read Online

ACCESS | Metrics & More | Article Recommendations | Supporting Information

ABSTRACT: We report a comprehensive experimental and computational study into low-frequency vibrational dynamics of hydroquinone clathrate during *in situ* gas loading, in order to monitor replacement of carbon dioxide with methane in its atomic-level pores. We used terahertz time-domain spectroscopy, because terahertz modes are highly sensitive to the identity and structure of enclathrated guest molecules. Through *ab initio* simulations, we determined that the replacement reaction is not completed. Instead we observed the formation of a heterogeneous material, with methane molecules occupying approximately one-third of available adsorption sites. While the structure of the methane-hydroquinone clathrate system has been previously determined, our observations suggest the reported symmetry is incorrect due to methane molecules weakly interacting with the framework, resulting in dynamic (as opposed to positional) disorder of guests, unlike the related fully ordered carbon dioxide clathrate. This work puts us on the path to quantitatively tracking gas loading in porous materials using terahertz spectroscopy.

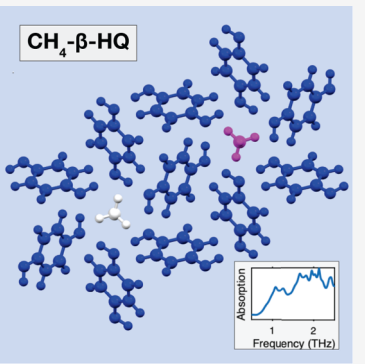

Clathrates are porous materials composed of cages of host molecules which are able to contain a small guest molecule, typically one per cage. For example, methane hydrates, a type of clathrate consisting of water ice as the host and methane as the guest, are abundant in the permafrost, composing a large portion of the world's hydrocarbon resources.[1] Under appropriate conditions of pressure and temperature, an enclathrated species can be replaced by a different guest molecule, thus sequestering a new species and freeing the original guest. In particular, the replacement reaction in which CO_2 replaces methane has attracted considerable attention, due to its relevance for both energy production and global climate change.[2] Replacement reactions are also important in other clathrate systems, such as organic clathrate formers such as hydroquinone (HQ), which has been studied for gas separation and hydrogen storage.[3−7] Replacement reactions in clathrate hydrates have been studied extensively using a variety of experimental techniques,[8−10] but reactions in hydroquinone clathrates are less well understood.[11]

In this paper, we describe experimental studies of the CH_4−CO_2 replacement reaction in HQ clathrates, using terahertz spectroscopy in a pressure cell.[12] We monitor the reaction *in situ* through the corresponding changes in the vibrational mode spectrum in the 0.5 THz to 2.5 THz range (corresponding to 15−84 cm^{-1}). Through comparisons with both density functional theory (DFT) calculations and *ab initio* molecular dynamics (AIMD) simulations, we confirm that, while previously published experiments and simulations have found that the CO_2 clathrate is fully ordered (both the framework and guest CO_2 molecules),[13] the guest methane molecules in *β*-HQ-CH_4 are not. There is little information related to the origin of such disorder, but it likely stems from the weak van der Waals interactions that exist between the methane molecules and the framework, which permit numerous orientations of the guest molecules to exist simultaneously, and in fact the published structure does not contain resolved CH_4 hydrogens.[14] This presents a challenge−and an opportunity−as the terahertz spectra of disordered materials are very different than those of ordered crystals.[15] Additionally, terahertz spectroscopy is able to differentiate between different types of disorder, as there would be a different response from materials where there exists positional disorder (i.e., the guest molecules are ordered but in different orientations across the bulk of the crystal) compared to dynamic disorder (i.e., where the guest molecules exhibit Brownian-type motions). We show that it is not possible to understand the spectra of these orientationally disordered clathrates by considering a linear combination of spectra from different ordered structures,[16] and instead only when the system is allowed to be dynamic do we recover the correct terahertz spectrum. This result has important fundamental implications, as the degree of guest

Received: April 23, 2024
Revised: May 23, 2024
Accepted: May 24, 2024

https://doi.org/10.1021/acs.jpclett.4c01188
J. Phys. Chem. Lett. 2024, 15, 6092−6098

ordering determines the coherence of long-range vibrational modes, which may play a role in mediating the replacement kinetics.[17] It also enables us to extract a rough estimate of the CO_2−CH_4 ratio in the system from terahertz spectra, for the first time.

Unlike water clathrates, HQ clathrates have the important advantage of room-temperature stability. Because of this, HQ has served as a valuable prototype for studying clathrate physics. HQ has four known polymorphs, labeled α through δ.[18,19] The α-polymorph is the most stable at room temperature and pressure, and is capable of enclathrating small molecules with one pore per 18 HQ molecules.[19] The β form can be accessed at elevated pressures, and is created via a phase transformation upon incorporation of guest molecules into the framework. β-HQ is the polymorph that is most often associated with HQ clathrates, with one pore for every three HQ molecules (see Figure 1). The γ- and δ-HQ forms are high-density polymorphs which do not form clathrates, and are not stable at standard conditions.[19] The γ form requires sublimation or evaporation, and the δ form requires very high pressure beyond the scope of our experiment.[18]

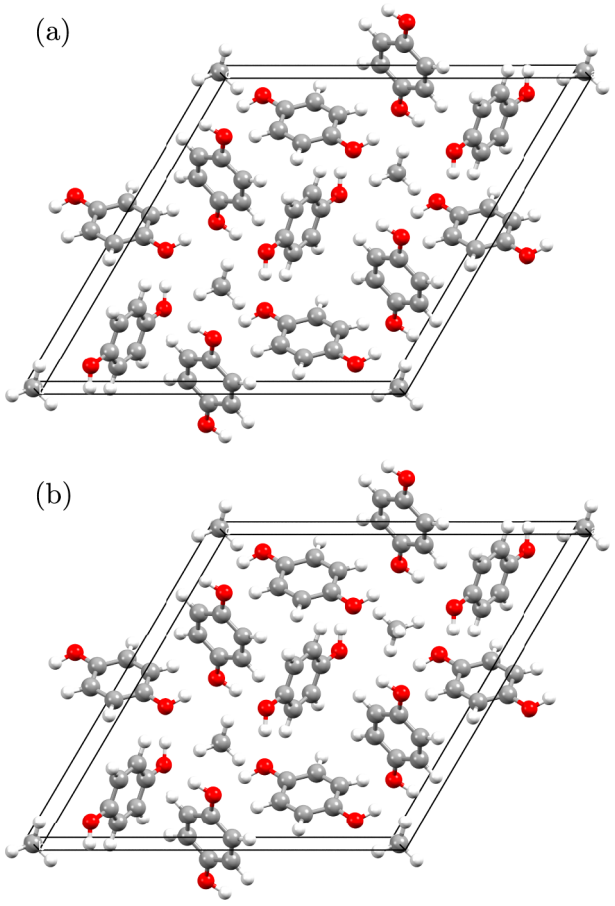

Figure 1. Unit cells for the space group $R3$ β-HQ-CH_4 (a) and the space group $P3$ β-HQ-CH_4 (b). Gray: carbon, white: hydrogen, red: oxygen.

β-HQ clathrates have been studied extensively with X-ray diffraction, Raman spectroscopy, and NMR.[5,20−22] In addition, recent work has established the value of terahertz spectroscopy for providing new insight into clathrate structure.[3] For example, previous studies have assigned the vibrational modes of β-HQ-CO_2 in the terahertz region.[13,17] The enclathration of CO_2 results in additional features in the experimental terahertz spectrum that arise from hindered translational motions of the guest CO_2 molecules within the pore. The frequency of this "cage-rattling" mode is strongly related to the strength of the noncovalent interactions between the HQ framework (host) and the CO_2 guest molecules. In addition, the combination of terahertz spectra and DFT simulations has indicated that the guest molecules can modify the structure and lattice dynamics of the clathrate through weak noncovalent forces, which can cause significant changes to the vibrational mode spectrum in the terahertz range.[13,17,23,24] Terahertz time-domain spectroscopy (THz-TDS) is therefore an excellent tool to apply to the study of replacement reactions, because of the strong relationship between these weak forces and the low-frequency vibrational modes of the structure.

We obtained α-HQ of purity ≥99.5% from Sigma-Aldrich and use it without modification, and confirmed the bulk purity through comparison with previously obtained THz-TDS data for α-HQ.[13,23] A quantity of approximately 40 mg was pressed into a 1 mm thick pellet of diameter 5 mm. Additionally, powdered high-density polyethylene (HDPE), also acquired commercially, was pressed into a pellet of the same dimensions. These two pellets were placed together inside a holder with a platinum mirror at the back. This holder was then inserted into a custom pressure cell, such that the terahertz beam could be quasi-optically coupled through a diamond window and the sample in a reflection geometry.[12] Because HDPE and HQ have very similar refractive indices in the terahertz range, of 1.54 and 1.6 respectively, there are no appreciable back-reflections from their interface.[25] However, unlike HQ, HDPE does not absorb much at terahertz frequencies. Therefore, the HDPE pellet was used to improve spectral resolution by increasing the terahertz path length, which delays a spurious time-domain reflection and thus allows us to use a longer time window in the data analysis.

To create β-HQ-CO_2, the cell chamber was pressurized to 5.5 MPa with CO_2 gas. Subsequently, following protocols from the literature for the conversion from α-HQ to β-HQ-CO_2, two heat cycles were performed between room temperature and 350 K, with the sample kept at each temperature for 1 h.[25] The transition from α-HQ to β-HQ-CO_2 can be confirmed by observing a large drop in the 1.6 THz peak characteristic of α-HQ, as previous work has shown.[13] Following the creation of β-HQ-CO_2, the connection to the CO_2 canister was then closed off, maintaining pressure within the cell. The chamber was reconnected to a CH_4 canister, some of the CO_2 was vented to avoid backflow, and then the connection was opened to the methane canister with an increased pressure of 8.3 MPa, without allowing the cell to return to atmospheric pressure at any point. The system was heat cycled twice more and then left pressurized and heated to 350 K for 24 h. This procedure initiates the replacement reaction.

Throughout the process, a THz-TDS spectrometer was used to monitor the terahertz spectrum of the sample within the pressure cell. This spectrometer acquired a complete time-resolved terahertz waveform consisting of the average of 3636 measurements every 10 min. This averaging time allowed us to resolve changes during heat cycles while also maintaining good dynamic range. The spectral resolution of these measurements, around 20 GHz, is limited by mandatory time-domain windowing of 12 ps needed to eliminate spurious reflections from the cell window. Our dynamic range enables determi-

https://doi.org/10.1021/acs.jpclett.4c01188
J. Phys. Chem. Lett. 2024, 15, 6092−6098

nation of accurate peak positions and amplitudes up to about 1.6 THz; the frequencies of peaks at higher frequencies can still be accurately obtained, but their amplitudes may be less accurate as they exceed the dynamic range of the measurement at these higher frequencies.[26] A transmission measurement of a 2 mm thick HDPE pellet, the same optical path length as through the HDPE pellet in the reflection geometry, was used as a standard reference to increase the dynamic range by avoiding the back reflections inherent to measurements within the cell.

Representative terahertz spectra are shown in Figure 2 (upper three curves). When comparing the blue trace labeled

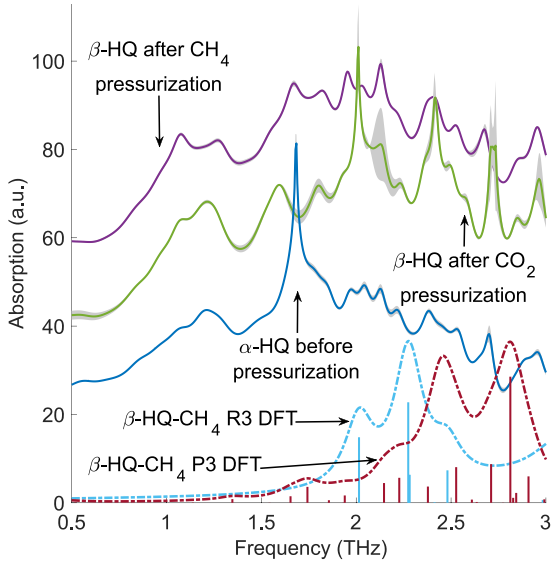

Figure 2. Experimental data of the entire replacement reaction, taking place over 46 h. Each curve represents the average of three 10-min measurements at room temperature, with the standard deviation overlaid in gray. Curves are offset by 20 along the y axis. The intensities of the simulated spectra are scaled globally to be comparable to the experimental absorption coefficients.

"α-HQ before pressurization" and the green trace labeled "β-HQ after CO_2 pressurization," we observe that the characteristic peak at 1.6 THz clearly present in the α-HQ spectrum drops sharply upon pressurization with CO_2 gas, indicating enclathration of CO_2 and the simultaneous transformation from α-HQ to β-HQ-CO_2, consistent with earlier studies.[17] After switching to CH_4 as the pressurizing medium, no change in the spectrum is observed until the first heating cycle. The spectrum shown after pressurization with CH_4 is shown in purple and labeled "β-HQ after CH_4 pressurization." The purple spectrum shows two peaks at 1.07 THz and 1.27 THz, with the 1.07 THz peak being slightly lower in amplitude than the 1.27 THz peak. The relative intensities of these two peaks switch during the heating cycles, until the system is maintained at 350 K for 24 h, after which cooling no longer switches the relative peak heights. Additionally, upon pressurization with CH_4, the peak which was at 1.21 THz prior to heating also exhibits a shift in frequency to 1.27 THz, further indicating a change to the system induced by the adsorption of CH_4. Since prior work has demonstrated that recovering α-HQ from β-HQ clathrate at a set temperature requires releasing the pressure, any peaks seen in the spectrum after heating are features of the new clathrate form rather than a return to α-HQ.[27] Thus, we conclude that at least some of the β-HQ-CO_2 has been converted to β-HQ-CH_4 at this point.

In order to interpret the experimental results, complementary numerical simulations are required. Simulations of (fully ordered) β-HQ-CO_2 have been performed earlier.[13,17] For the methane clathrate, we rely on the experimental crystal structure for β-HQ-CH_4[14] (Cambridge Crystallographic Data Centre (CCDC) database reference code: QOLWUM), which was used as the starting point for all calculations. This reported structure belongs to the $R\bar{3}$ space group with cell parameters $a = b = 16.207$ Å, $c = 5.780$ Å. However, that structure does not report methane hydrogen positions, which must be determined in order to perform full vibrational analyses. Importantly, it is not possible to utilize the reported space group with ordered methane molecules (including hydrogens), as the $R\bar{3}$ symmetry operators will always introduce disorder in the individual methanes. Therefore, an initial search for ordered structures that conform to lower-symmetry space groups was performed. Since the published structure only contains one pore per unit cell, a supercell was generated to allow for multiple different orientations of the methane molecules within the pore, i.e., the removal of the translational symmetry constraint. CH_4 molecules were placed into the three pores within a single crystalline unit cell with varying orientations. Multiple possible configurations of the methane molecules, in the absence of any space group symmetry, were generated. Subsequently, the structural models were optimized using the solid-state software CP2K (version 9.0),[28,29] while taking into account the periodicity of the system.[30,31] The Becke-Lee−Yang−Parr (BLYP) generalized gradient approximation functional,[32,33] alongside Grimme's D3 dispersion correction[34−36] were used for all simulations. The Goedecker-Teter-Hutter (GTH) pseudopotentials[34,37,38] were also used with the double-ζ DZVP-MOLOPT[39,40] basis set.

An energy analysis of the resulting structures indicates that there are two structures that were ca. 4 kJ mol^{-1} lower in energy than the others, which were subjected to a symmetry analysis to uncover crystallographic symmetry. These two structures, shown in Figure 1, belong to the $R3$ and $P3$ space groups, respectively. They mainly differ in the orientations of the methane guest molecules with the structure in the $R3$ space group having the two methane molecules in identical orientations, while the two molecules are related by inversion symmetry in the $P3$ structure. These two structures were subjected to complete geometry optimizations (all lattice vectors and atomic positions allowed to relax within the space group symmetry of the crystal), with the only constraint being the preservation of the identified space group symmetry of the solid-lattice vectors, using the CRYSTAL23 software package.[41] This yields nearly identical lattice vectors for the two structures: $a = b = 16.451$ Å, $c = 5.421$ Å, for the $R3$ structure, and $a = b = 16.462$ Å, $c = 5.412$ Å, for the $P3$ structure. Importantly, these structures have nearly the same energy on a per unit cell basis ($\Delta E = 0.00533$ kJ $mol^{-1} = 0.055$ meV), which is unsurprising given that the only interaction between the methane molecules and the framework arises from weak dispersion forces. Such a low energy difference implies that both structures have an equal probability of being present in a sample, down to temperatures as low as 2 K.

Subsequently, fully static (0 K) vibrational simulations were performed within the harmonic approximation via finite-differences and numerical differentiation using the CRYSTAL23 software package, which yielded vibrational normal modes

https://doi.org/10.1021/acs.jpclett.4c01188
J. Phys. Chem. Lett. 2024, 15, 6092−6098

(eigenvectors) and frequencies (eigenvalues).[41−43] CRYSTAL23 was chosen for the static-DFT vibrational analyses given its long track record for successfully simulating the terahertz spectra of molecular crystals.[44−47] Here, we have attempted to mimic the theoretical parameters used by the CP2K simulations as much as possible given the differences inherent to the two codes, by utilizing the generalized gradient approximation (GGA) Perdew−Burke−Ernzerhof (PBE)[48] functional coupled with Grimme's D3 dispersion correction[35,36] and the Ahlrichs TZVP basis set.[49] Infrared intensities were determined through the Berry Phase method.[50]

Despite the minute differences in energy and overall lattice dimensions, the predicted terahertz spectra of the two structures are clearly distinct (Figure 2, lower two curves). While the spectrum of the *P*3 structure exhibits multiple peaks, with some below 2 THz, the *R*3 structure does not exhibit any absorption features below 2 THz. It is important to note that these differences do not simply arise due to differences in the space group symmetry, as there are a number of modes predicted in the *P*3 structure that do not exist at all in the *R*3 simulation, indicating that it is due to the different long-range forces present in the materials (see Supporting Information for a full list of vibrational modes and IR activities). Indeed, this can be observed in the calculated thermodynamic parameters, which predict the *R*3 structure to have a relative stabilization of the Gibbs energy at 300 K of 4.46 kJ mol^{-1} (due to entropic effects), while the structures have nearly the same energy at 0 K. This result highlights the extreme sensitivity of terahertz spectroscopy to the supramolecular arrangement of atoms and molecules in the condensed phase—even when the intermolecular forces are of some of the weakest varieties.

Evidently, neither of these predicted spectra from the completely ordered β-HQ-CH_4 models are in agreement with the experimental THz-TDS data. In particular, we note the absorption feature at around 1 THz, which increases in intensity upon CH_4 loading, indicating that this mode is influenced by the presence of CH_4 molecules (Figure 3).

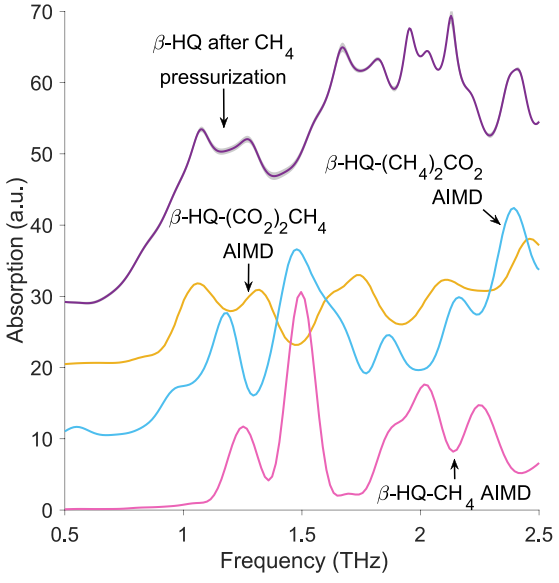

Figure 3. Final state of β-HQ-CH_4 in purple compared to AIMD simulations of β-HQ-$(CO_2)_2CH_4$ in yellow, β-HQ-$(CH_4)_2$-CO_2 in blue, and β-HQ-CH_4 in pink. Curves are offset by 10 au along the *y* axis.

Because of the very weak interaction between the guest methanes and the host framework, it seems likely that the physical structure of β-HQ-CH_4 contains truly disordered methane molecules. To explore this possibility, we performed AIMD simulations with CP2K, which do not take advantage of space group symmetry, on both of the structures previously analyzed using static-DFT simulations, because CRYSTAL23 does not contain a molecular dynamics module. The simulations were run within the NVT ensemble, with a time-step of 0.5 fs and with the temperature set to 100 K to preserve any possible structural ordering and to compare to the experimental THz-TDS results. In both simulations, the guest methane molecules immediately began to rotate freely within the guest sites, and no structural ordering or coupling between adjacent methane molecules was observed, which indicates that the structure is indeed fully disordered, even at low temperatures—in line with the energetic analysis using the static-DFT simulations.

This result highlights a possible reason for the failure of the static-DFT simulations to capture the observed lattice dynamics from the THz-TDS experiments: the lack of inclusion of methane disorder. Given that there are dramatic differences in the predicted terahertz spectra for the two proposed ordered structures, it can be reasonably expected that disordered structures would have their own unique terahertz spectrum as well.

To explore this idea, an IR spectrum was generated from the AIMD trajectory by determining the dipole moments for each AIMD frame through the Voronoi integration approach of the volumetric electron density.[51] Using the TRAVIS analyzer, the dipole moment autocorrelation function was used to generate an IR spectrum. The resulting spectrum, shown in Figure 3 (bottom curve), is markedly different from the static-DFT vibrational results (shown above in Figure 2)—in particular, the static-DFT (ordered) spectra contain no vibrational modes below ca. 1.6 THz, while the disordered AIMD spectra exhibit at least two features below 1.5 THz. This showcases the utility of low-frequency vibrational spectroscopy for exploring these types of systems over conventional structural methods. As the vast majority of diffraction studies provide a dynamically averaged picture of the atomic-level structure, it is difficult to extract the nature of solid-state disorder directly without additional techniques. However, since weak intermolecular forces are what dictate different types of disorder in solids, terahertz spectroscopy is able to differentiate them.

The final step in our analysis is informed by recent studies on HQ clathrates, which suggested that CO_2−CH_4 replacement reactions are generally incomplete, leaving both guest molecules present in the final system.[11,14] In fact, ref 11 reports that the replacement reaction from CO_2 to CH_4 resulted in only 6% to 9% of CO_2 molecules replaced. However, if even a small proportion of CO_2 molecules are replaced in the clathrate, we expect a measurable impact on the resulting spectra because terahertz spectroscopy is so sensitive to the identity and orientation of the guest molecules.[46,52]

Accordingly, since AIMD simulations of neither pure CO_2 nor pure CH_4 fully explain spectral features like the relative heights of the 1.07 THz peak and the 1.21 THz peak, we initialized simulations of mixed-gas states, where some pores are occupied by CO_2 and others by CH_4 molecules. We generated supercells with proportions of two-to-one and one-to-two CH_4-to-CO_2, respectively, corresponding to the options for a system with three pores per unit cell. These two mixed-state simulated spectra (Figure 3 middle two curves) show

https://doi.org/10.1021/acs.jpclett.4c01188
J. Phys. Chem. Lett. 2024, 15, 6092−6098

marked differences from the pure states. While the peak at 1.5 THz from the pure CH_4 state is retained in the two-to-one CH_4-to-CO_2 spectrum, it is completely absent in the one-to-two CH_4-to-CO_2 spectrum. Furthermore, both spectra exhibit a peak slightly below 1 THz which is not present in either pure spectrum. Higher frequency modes are also very distinct, with the 2 THz peak in the pure CH_4 spectrum absent in both mixed states, and the CO_2 spectrum showing only two peaks between 1.5 and 2 THz while the other spectra have three or more.

These mixed-state simulations are a much better match to the experimental data. The features at 1.07 THz and 1.21 THz are duplicated in the one-to-two CH_4-to-CO_2 AIMD simulation (Figure 3 yellow curve), including their switched relative peak heights compared to the pure CO_2 spectrum. In addition, the feature near 1.8 THz also shows a better match to the measurements. As a result, we conclude that the final state in our experiments is likely a mixed clathrate with an approximate ratio of one methane molecule to two CO_2 molecules. To our knowledge, this is the first example of a mixture ratio determination in a porous system based on terahertz vibrational spectroscopy.

We have studied a prototype replacement reaction in HQ clathrate using THz-TDS as well as DFT and AIMD simulations. Our results indicate that the methane in the pores is highly disordered. THz-TDS is the ideal tool for studying this disorder because of the exquisite sensitivity of the low-frequency vibrational spectrum to small differences in bulk structure and weak interactions between host and guest molecules. By comparing measured spectra with those extracted from AIMD simulations, we also determine that not all of the CO_2 is released from the HQ pores, resulting in a mixed state with both CH_4 and CO_2 guests in the clathrate. These simulations allow a rough estimate of the mixture ratio, based on the agreement with various spectral features in the 0.5−2.0 THz range. The final mixture contains at least some CH_4, but less than two-thirds, with a reasonable match to the simulated AIMD spectrum which includes one-third CH_4 and two-thirds CO_2. Such findings highlight the importance of utilizing appropriate theoretical methods to understand the fundamental physics associated with crystalline disorder, and how standardized methods (static-DFT) are not appropriate for understanding the terahertz dynamics for such systems, necessitating development of new techniques. These results demonstrate the possibility of using low-frequency vibrational spectroscopy in the terahertz range for quantitative assessment of host−guest complexes with mixed occupancies.

■ ASSOCIATED CONTENT

Supporting Information

The Supporting Information is available free of charge at https://pubs.acs.org/doi/10.1021/acs.jpclett.4c01188.

Diagram of the experimental setup, a unit cell diagram of β-HQ-CO_2, additional spectra from pressurized measurements, the dynamic range calculation, and a table of DFT-simulated mode frequencies (PDF)

■ AUTHOR INFORMATION

Corresponding Author

Katharine D. Bancroft − *Department of Physics, Brown University, Providence, Rhode Island 02912, United States;* orcid.org/0009-0007-9091-8884; Email: katharine_bancroft@brown.edu

Authors

Saheed A. Ajibade − *Department of Chemistry, University of Vermont, Burlington, Vermont 05405, United States*

Johanna Kölbel − *School of Engineering, Brown University, Providence, Rhode Island 02912, United States;* orcid.org/0000-0002-9820-1892

Michael T. Ruggiero − *Department of Chemistry, University of Rochester, Rochester, New York 14627, United States;* orcid.org/0000-0003-1848-2565

Daniel M. Mittleman − *School of Engineering, Brown University, Providence, Rhode Island 02912, United States;* orcid.org/0000-0003-4277-7419

Complete contact information is available at: https://pubs.acs.org/10.1021/acs.jpclett.4c01188

Notes

The authors declare no competing financial interest.

■ ACKNOWLEDGMENTS

MTR and SA thank the National Science Foundation (award NSF-2055402). KDB, JK, and DMM acknowledge the support of the National Science Foundation (NSF-2055417) and the Hibbitt Postdoctoral Fellows Program.

■ REFERENCES

(1) Sloan, E. D. Fundamental Principles and Applications of Natural Gas Hydrates. *Nature* **2003**, *426*, 353−359.

(2) Goel, N. In Situ Methane Hydrate Dissociation with Carbon Dioxide Sequestration: Current Knowledge and Issues. *J. Petrol. Sci. Eng.* **2006**, *51*, 169−184.

(3) Lee, Y.-J.; Han, K. W.; Jang, J. S.; Jeon, T.-I.; Park, J.; Kawamura, T.; Yamamoto, Y.; Sugahara, T.; Vogt, T.; Lee, J.-W.; Lee, Y.; Yoon, J.-H. Selective CO_2 Trapping in Guest-Free Hydroquinone Clathrate Prepared by Gas-Phase Synthesis. *ChemPhysChem* **2011**, *12*, 1056−1059.

(4) Coupan, R.; Péré, E.; Dicharry, C.; Plantier, F.; Diaz, J.; Khoukh, A.; Allouche, J.; Labat, S.; Pellerin, V.; Grenet, J.-P.; Sotiropoulos, J.-M.; Senechal, P.; Guerton, F.; Moonen, P.; Torré, J.-P. Characterization Study of CO_2, CH_4, and CO_2/CH_4 Hydroquinone Clathrates Formed by Gas−Solid Reaction. *J. Phys. Chem. C* **2017**, *121*, 22883−22894.

(5) Coupan, R.; Péré, E.; Dicharry, C.; Torré, J.-P. New Insights on Gas Hydroquinone Clathrates Using in Situ Raman Spectroscopy: Formation/Dissociation Mechanisms, Kinetics, and Capture Selectivity. *J. Phys. Chem. A* **2017**, *121*, 5450−5458.

(6) Sun, N.; Li, Y.; Qiu, N.; Liu, Z.; Francisco, J. S.; Du, S. Adsorption Behaviors for Clathrate Hydrates of CO2 with Mixed Gases. *Fuel* **2024**, *358*, 130265.

(7) Daschbach, J. L.; Chang, T.-M.; Corrales, L. R.; Dang, L. X.; McGrail, P. Molecular Mechanisms of Hydrogen-Loaded β-Hydroquinone Clathrate. *J. Phys. Chem. B* **2006**, *110*, 17291−17295.

(8) Murshed, M. M.; Schmidt, B. C.; Kuhs, W. F. Kinetics of Methane-Ethane Gas Replacement in Clathrate-Hydrates Studied by Time-Resolved Neutron Diffraction and Raman Spectroscopy. *J. Phys. Chem. A* **2010**, *114*, 247−255.

(9) Yang, M.; Chong, Z. R.; Zheng, J.; Song, Y.; Linga, P. Advances in Nuclear Magnetic Resonance (NMR) Techniques for the Investigation of Clathrate Hydrates. *Renew. Sustain. Energy Rev.* **2017**, *74*, 1346−1360.

(10) Komatsu, H.; Ota, M.; Smith, R. L.; Inomata, H. Review of CO2−CH4 Clathrate Hydrate Replacement Reaction Laboratory Studies − Properties and Kinetics. *J. Taiwan Inst. Chem. E* **2013**, *44*, 517−537.

(11) Yoon, S. J.; Lee, D.; Yoon, J.-H.; Lee, J.-W. Swapping and Enhancement of Guest Occupancies in Hydroquinone Clathrates Using CH_4 and CO_2. *Energy Fuels* **2019**, *33*, 6634−6640.
(12) Zhang, W.; Nickel, D.; Mittleman, D. High-Pressure Cell for Terahertz Time-Domain Spectroscopy. *Opt. Express* **2017**, *25*, 2983−2993.
(13) Zhang, W.; Song, Z.; Ruggiero, M. T.; Mittleman, D. M. Assignment of Terahertz Modes in Hydroquinone Clathrates. *J. Infrared Millim. Terahertz Waves* **2020**, *41*, 1355−1365.
(14) Torré, J.-P.; Gornitzka, H.; Coupan, R.; Dicharry, C.; Pérez-Rodríguez, M.; Comesaña, A.; Piñeiro, M. M. Insights into the Crystal Structure and Clathration Selectivity of Organic Clathrates Formed with Hydroquinone and (CO_2 + CH_4) Gas Mixtures. *J. Phys. Chem. C* **2019**, *123*, 14582−14590.
(15) Walther, M.; Fischer, B. M.; Jepsen, P. U. Noncovalent Intermolecular Forces in Polycrystalline and Amorphous Saccharides in the Far Infrared. *Chem. Phys.* **2003**, *288*, 261−268.
(16) Nickel, D. V.; Ruggiero, M. T.; Korter, T. M.; Mittleman, D. M. Terahertz Disorder-Localized Rotational Modes and Lattice Vibrational Modes in the Orientationally-Disordered and Ordered Phases of Camphor. *Phys. Chem. Chem. Phys.* **2015**, *17*, 6734−6740.
(17) Zhang, W.; Song, Z.; Ruggiero, M. T.; Mittleman, D. M. Terahertz Vibrational Motions Mediate Gas Uptake in Organic Clathrates. *Cryst. Growth. Des.* **2020**, *20*, 5638−5643.
(18) Naoki, M.; Yoshizawa, T.; Fukushima, N.; Ogiso, M.; Yoshino, M. A New Phase of Hydroquinone and Its Thermodynamic Properties. *J. Phys. Chem. B* **1999**, *103*, 6309−6313.
(19) Wallwork, S. C.; Powell, H. M. The Crystal Structure of the α Form of Quinol. *J. Chem. Soc., Perkin Trans.* **1980**, *2*, 641−646.
(20) Boeyens, J. C. A.; Pretorius, J. A. X-ray and Neutron Diffraction Studies of the Hydroquinone Clathrate of Hydrogen Chloride. *Acta Crystall. B-Stru.* **1977**, *33*, 2120−2124.
(21) Lee, J.-W.; Choi, K. J.; Lee, Y.; Yoon, J.-H. Spectroscopic Identification and Conversion Rate of Gaseous Guest-Loaded Hydroquinone Clathrates. *Chem. Phys. Lett.* **2012**, *528*, 34−38.
(22) Lee, J.-W.; Lee, S. H.; Yoon, S. J.; Yoon, J.-H. Spectroscopic Investigation, Cage Occupancy, and Gas Storage Capacity of Hydroquinone Clathrates Formed with H_2S-N_2 and COS-N_2 Binary Gas Mixtures. *Korean J. Chem. Eng.* **2017**, *34*, 2710−2714.
(23) Zhang, W.; Maul, J.; Vulpe, D.; Moghadam, P. Z.; Fairen-Jimenez, D.; Mittleman, D. M.; Zeitler, J. A.; Erba, A.; Ruggiero, M. T. Probing the Mechanochemistry of Metal−Organic Frameworks with Low-Frequency Vibrational Spectroscopy. *J. Phys. Chem. C* **2018**, *122*, 27442−27450.
(24) Takeya, K.; Zhang, C.; Kawayama, I.; Murakami, H.; Jepsen, P. U.; Chen, J.; Wu, P.; Ohgaki, K.; Tonouchi, M. Terahertz Time Domain Spectroscopy for Structure-II Gas Hydrates. *Appl. Phys. Express* **2009**, *2*, 122303.
(25) Jang, J. S.; Jeon, T.-I.; Lee, Y.-J.; Yoon, J.-H.; Lee, Y. Characterization of α-Hydroquinone and β-Hydroquinone Clathrates by THz Time-Domain Spectroscopy. *Chem. Phys. Lett.* **2009**, *468*, 37−41.
(26) Jepsen, P. U.; Fischer, B. M. Dynamic Range in Terahertz Time-Domain Transmission and Reflection Spectroscopy. *Opt. Lett.* **2005**, *30*, 29−31.
(27) Lee, E. S.; Han, K. W.; Yoon, J.-H.; Jeon, T.-I. Probing Structural Transition and Guest Dynamics of Hydroquinone Clathrates by Temperature-Dependent Terahertz Time-Domain Spectroscopy. *J. Phys. Chem. A* **2011**, *115*, 35−38.
(28) Kühne, T. D.; et al. CP2K: An Electronic Structure and Molecular Dynamics Software Package - Quickstep: Efficient and Accurate Electronic Structure Calculations. *J. Chem. Phys.* **2020**, *152*, 194103.
(29) VandeVondele, J.; Krack, M.; Mohamed, F.; Parrinello, M.; Chassaing, T.; Hutter, J. Quickstep: Fast and Accurate Density Functional Calculations Using a Mixed Gaussian and Plane Waves Approach. *Comput. Phys. Commun.* **2005**, *167*, 103−128.
(30) Dovesi, R.; Erba, A.; Orlando, R.; Zicovich-Wilson, C. M.; Civalleri, B.; Maschio, L.; Rérat, M.; Casassa, S.; Baima, J.; Salustro, S.; Kirtman, B. Quantum-Mechanical Condensed Matter Simulations with CRYSTAL. *WIREs Comput. Mol. Sci.* **2018**, *8*, e1360.
(31) Banks, P. A.; Burgess, L.; Ruggiero, M. T. The Necessity of Periodic Boundary Conditions for the Accurate Calculation of Crystalline Terahertz Spectra. *Phys. Chem. Chem. Phys.* **2021**, *23*, 20038−20051.
(32) Becke, A. D. Density-Functional Exchange-Energy Approximation with Correct Asymptotic Behavior. *Phys. Rev. A* **1988**, *38*, 3098−3100.
(33) Lee, C.; Yang, W.; Parr, R. G. Development of the Colle-Salvetti Correlation-Energy Formula into a Functional of the Electron Density. *Phys. Rev. B* **1988**, *37*, 785−789.
(34) Grimme, S. Accurate Description of van der Waals Complexes by Density Functional Theory including Empirical Corrections. *J. Comput. Chem.* **2004**, *25*, 1463−1473.
(35) Grimme, S.; Hansen, A.; Brandenburg, J. G.; Bannwarth, C. Dispersion-Corrected Mean-Field Electronic Structure Methods. *Chem. Rev.* **2016**, *116*, 5105−5154.
(36) Grimme, S.; Antony, J.; Ehrlich, S.; Krieg, H. A Consistent and Accurate Ab Initio Parametrization of Density Functional Dispersion Correction (DFT-D) for the 94 Elements H-Pu. *J. Chem. Phys.* **2010**, *132*, 154104.
(37) Goedecker, S.; Teter, M.; Hutter, J. Separable Dual-Space Gaussian Pseudopotentials. *Phys. Rev. B* **1996**, *54*, 1703−1710.
(38) Hartwigsen, C.; Goedecker, S.; Hutter, J. Relativistic Separable Dual-Space Gaussian Pseudopotentials from H to Rn. *Phys. Rev. B* **1998**, *58*, 3641−3662.
(39) VandeVondele, J.; Hutter, J. Gaussian Basis Sets for Accurate Calculations on Molecular Systems in Gas and Condensed Phases. *J. Chem. Phys.* **2007**, *127*, 114105.
(40) VandeVondele, J.; Hutter, J. An Efficient Orbital Transformation Method for Electronic Structure Calculations. *J. Chem. Phys.* **2003**, *118*, 4365−4369.
(41) Erba, A.; Desmarais, J. K.; Casassa, S.; Civalleri, B.; Donà, L.; Bush, I. J.; Searle, B.; Maschio, L.; Edith-Daga, L.; Cossard, A.; Ribaldone, C.; Ascrizzi, E.; Marana, N. L.; Flament, J.-P.; Kirtman, B. CRYSTAL23: A Program for Computational Solid State Physics and Chemistry. *J. Chem. Theory Comput.* **2023**, *19*, 6891−6932.
(42) Zicovich-Wilson, C. M.; Pascale, F.; Roetti, C.; Saunders, V. R.; Orlando, R.; Dovesi, R. Calculation of the Vibration Frequencies of α-Quartz: The Effect of Hamiltonian and Basis Set. *J. Comput. Chem.* **2004**, *25*, 1873−1881.
(43) Pascale, F.; Zicovich-Wilson, C. M.; López Gejo, F.; Civalleri, B.; Orlando, R.; Dovesi, R. The Calculation of the Vibrational Frequencies of Crystalline Compounds and Its Implementation in the CRYSTAL Code. *J. Comput. Chem.* **2004**, *25*, 888−897.
(44) Ruggiero, M. T.; Sutton, J. J.; Fraser-Miller, S. J.; Zaczek, A. J.; Korter, T. M.; Gordon, K. C.; Zeitler, J. A. Revisiting the Thermodynamic Stability of Indomethacin Polymorphs with Low-Frequency Vibrational Spectroscopy and Quantum Mechanical Simulations. *Cryst. Growth Des.* **2018**, *18*, 6513−6520.
(45) Li, Q.; Zaczek, A. J.; Korter, T. M.; Zeitler, J. A.; Ruggiero, M. T. Methyl-Rotation Dynamics in Metal-Organic Frameworks Probed with Terahertz Spectroscopy. *Chem. Commun.* **2018**, *54*, 5776−5779.
(46) Li, Q.; Kölbel, J.; Davis, M. P.; Korter, T. M.; Bond, A. D.; Threlfall, T.; Zeitler, J. A. In Situ Observation of the Structure of Crystallizing Magnesium Sulfate Heptahydrate Solutions with Terahertz Transmission Spectroscopy. *Cryst. Growth. Des.* **2022**, *22*, 3961−3972.
(47) Li, Q.; Bond, A. D.; Korter, T. M.; Zeitler, J. A. New Insights into the Crystallographic Disorder in the Polymorphic Forms of Aspirin from Low-Frequency Vibrational Analysis. *Mol. Pharmaceutics* **2022**, *19*, 227−234.
(48) Paier, J.; Hirschl, R.; Marsman, M.; Kresse, G. The Perdew−Burke−Ernzerhof Exchange-Correlation Functional Applied to the G2−1 Test Set Using a Plane-Wave Basis Set. *J. Chem. Phys.* **2005**, *122*, 234102.

https://doi.org/10.1021/acs.jpclett.4c01188
J. Phys. Chem. Lett. 2024, 15, 6092−6098

(49) Schäfer, A.; Huber, C.; Ahlrichs, R. Fully Optimized Contracted Gaussian Basis Sets of Triple Zeta Valence Quality for Atoms Li to Kr. *J. Chem. Phys.* **1994**, *100*, 5829−5835.
(50) Noel, Y.; Zicovich-Wilson, C. M.; Civalleri, B.; D'Arco, Ph.; Dovesi, R. Polarization Properties of ZnO and BeO: An Ab Initio Study through the Berry Phase and Wannier Functions Approaches. *Phys. Rev. B* **2001**, *65*, 014111.
(51) Brehm, M.; Kirchner, B. TRAVIS - A Free Analyzer and Visualizer for Monte Carlo and Molecular Dynamics Trajectories. *J. Chem. Inf. Model.* **2011**, *51*, 2007−2023.
(52) Ajibade, S.; Catalano, L.; Kölbel, J.; Mittleman, D.; Ruggiero, M. Terahertz Spectroscopy Unambiguously Determines the Orientation of Guest Water Molecules in a Structurally Elusive Metal−Organic Framework. *J. Phys. Chem. Lett.* **2024**, *15*, 5549−5555.

https://doi.org/10.1021/acs.jpclett.4c01188
J. Phys. Chem. Lett. 2024, 15, 6092−6098